Modeling and Simulation of Shielded Microstrip Lines

by

Sarhan M. Musa and Matthew N.O. Sadiku
College of Engineering
Prairie View A&M University, Prairie View, Texas 77446
smmusa, mnsadiku,@pvamu.edu

Abstract: *Microstrip lines are the most commonly used transmission lines at high frequencies. Modeling and simulation of microstrip lines becomes essential technique to investigate. In this paper, we illustrate how to model and simulate the capacitance of rectangular coaxial lines using COMSOL, a finite element software. We also determine the capacitance coupling of the single-strip, double-strip, three-strip, six-strip, and eight-strip shielded microstrip lines. We compared our results with those obtained by other methods and found them to be close.*

***Keywords**:* Shielded microstrip lines, Rectangular coaxial lines, Capacitance per unit length, Multiconductor transmission lines, Modeling and simulation.

I. Introduction

Today, electromagnetic propagation on multiple parallel transmission lines has been a very attractive area in computational electromagnetics. Multiple parallel transmission lines have been successfully applied and used by designers in compact packaging, semiconductor device, high speed interconnecting buses, monolithic integrated circuits, and other applications.

Microstrip lines are the most commonly used in all planar circuits despite of the frequencies ranges of the applied signals. Microstrip lines are the most commonly used transmission lines at high frequencies. Quasi-static analysis of microstrip lines involves evaluating them as parallel plates transmission lines, supporting a pure "TEM" mode.

Development in microwave circuits using rectangular coaxial lines as transmission medium has been improving over the past decades [1]. Reid and Webster used rectangular coaxial transmission lines to fabricate a 60 GHz branch line coupler [2]. Xu and Zhou used the finite difference time domain method for analyzing satellite beamforming network consisting of rectangular coaxial line [3].

Advances in microwave solid-state devices have stimulated interest in the integration of microwave circuits. Today, microstrip transmission lines have attracted great attention and interest in microwave integrated circuit applications. This creates the need for accurate modeling and simulation of microstrip transmission lines. Due to the difficulties associated with analytical methods [4-7] for calculating the capacitance of shielded microstrip transmission lines, other methods have been applied. Such methods include finite difference technique, extrapolation [7], point-matching method [8], boundary element method [9], spectral-space domain method [10], finite element method [11-13], conformal mapping method [14], transverse modal analysis [15], and mode-matching method [16].

In this paper, we consider systems of rectangular coaxial lines as well as single-strip, double-strip, three-strip, six-strip, and eight-strip (multiconductor) shielded microstrip lines. Using COMSOL [17], a finite element package, we performed the simulation of these systems of microstrip lines. We compared the results with other methods and found them to be in good agreement.

II. Discussions and Results

The rectangular coaxial line consists of a two-conductor transmission system along which TEM wave propagates. The characteristic impedance of such a lossless line is given by

$$Z = \sqrt{\frac{L}{C}} = \frac{1}{cC} \qquad (1)$$

where

Z = characteristic impedance of the line
L = inductance per unit length of the line
C = capacitance per unit length of the line
$c = 3 \times 10^8$ m/s (the speed of light in vacuum)

As shown in Fig. 1, a rectangular coaxial line consists of inner and outer rectangular conductors with a dielectric material separating them.

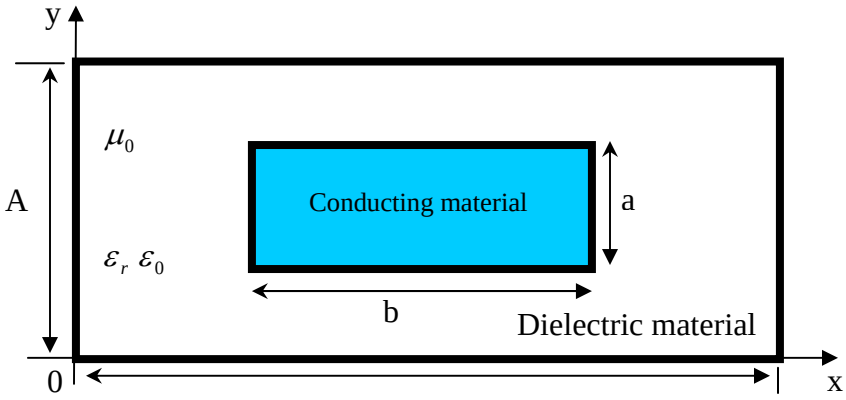

Figure 1. Cross-section of the rectangular coaxial line.

Using COMSOL [17] for each type of the rectangular lines involves taking the following steps:

1. Develop the geometry of the inner and outer conductors, such as shown in Fig. 2.

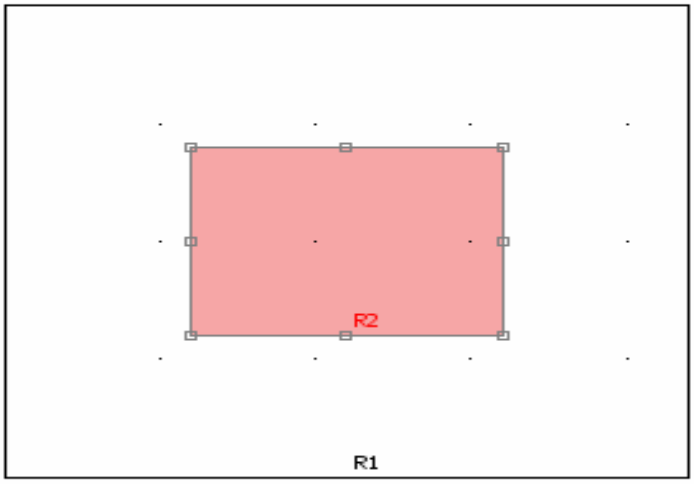

Figure 2. Geometry of the rectangular coaxial line model.

2. Select both conductors/rectangle and take the difference.
3. We select the relative permittivity as 1 for the difference in step 2. For the boundary, we select the outer conductor as ground and inner conductor as port.
4. We generate the finite element mesh as in Fig. 3.

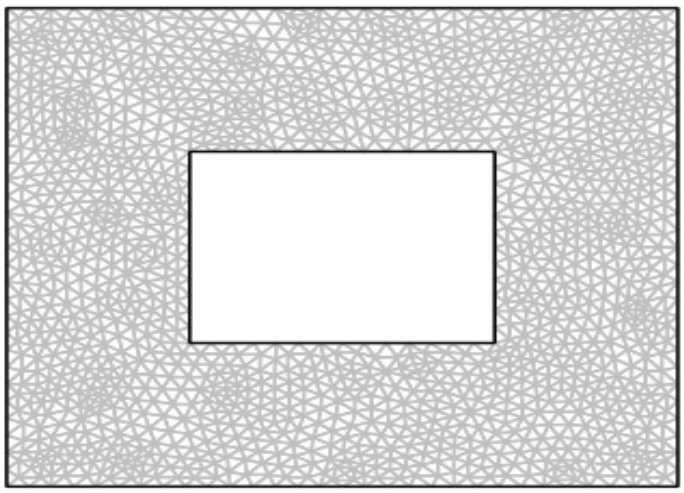

Figure 3. Mesh of the rectangular coaxial line.

5. We solve the model and obtain the potential shown in Fig. 4.

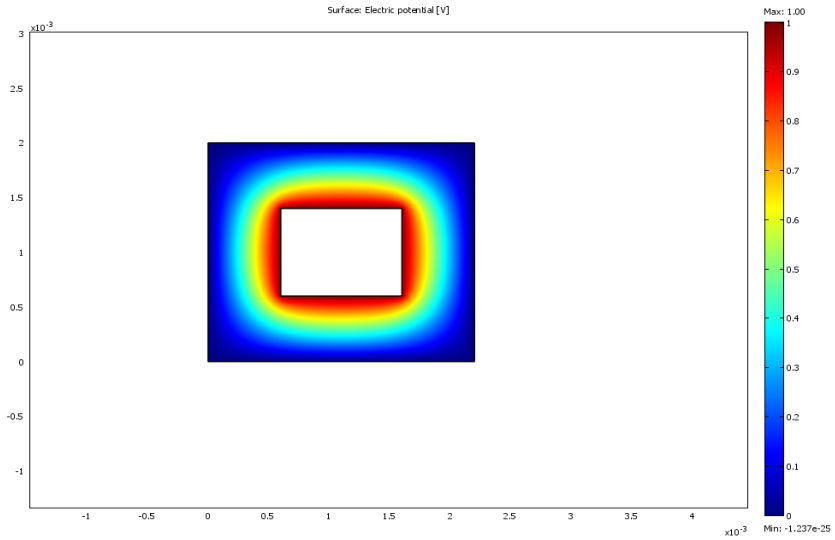

Figure 4. Image for the Potential distribution of the rectangular coaxial line.

6. As postprocessing, we select Point Evaluation and choose capacitance element 11 to find the capacitance per unit length of the line.

We now consider the following three models.

A. Rectangular cross-section transmission line

For COMSOL, we use the following values.
Dielectric material:
ε_r =1, μ_r =1,σ = 0 S/m (air)
Conducting material:

ε_r =1, μ_r =1,σ = 5.8 x 10^7 S/m (copper)
where

ε_0 = permittivity of free space = $\frac{1}{36\pi}\times 10^{-9} = 8.854\times 10^{-12}$ F/m

ε_r = dielectric constant

μ_r = relative permeability

μ_0 = permeability of free space = $4\pi\times 10^{-7} = 1.257\times 10^{-6}$ H/m

σ = conductivity of the conductor

a = width of the inner conductor = 1 mm
b = height of the inner conductor = 0.8 mm
A= width of the outer conductor = 2.2 mm
B = height of the outer conductor = 2 mm

From the COMSOL model, we obtained the capacitance per unit length (based on the dimensions given above) as 72.94 pF/m. Using the finite difference (FD) method, we obtained the capacitance per unit length of the line as 71.51 pF/m. Table 1 shows the comparison of the characteristic impedance (using eq. 1) of several models. It is evident from the table that the results are very close.

Table 1 Comparison of characteristic impedance Values of rectangular coaxial line.

Name	Z_0
Zheng et al. [18]	45.789
Chen [19]	45.759
Costamagna and Fanni [20]	45.767
Lau [21]	45.778
Finite difference (FD) [22]	46.612
COMSOL [17]	45.70

B. Square cross-section transmission line

This is only a special case of the rectangular line. We used the same values for the dielectric and conducting materials. We used the following dimensions for the line.

a = width of the inner conductor = 2 mm
b = height of the inner conductor = 2 mm
A= width of the outer conductor = 4 mm
B = height of the outer conductor = 4 mm

From the COMSOL model, we obtained the capacitance per unit length as 90.696 pF/m. Using the finite difference (FD) method [22], we obtained the capacitance per unit length of the line as 90.714 pF/m. Table 2 presents the comparison of the characteristic

impedance of several models. It is evident from the table that the results are in good agreement.

Table 2 Comparison of characteristic impedance Values of square coaxial line.

Name	Z_0
Zheng et al. [18]	36.79
Lau [21]	36.81
Cockcroft [23]	36.80
Bowan [24]	36.81
Green [25]	36.58
Ivanov and Djankov [26]	36.97
Costamagna and Fanni [20]	36.81
Riblet [27]	36.80
Finite difference (FD) [22]	36.75
COMSOL [17]	36.75

C. Rectangular line with Diamondwise structure:

The geometry of the cross-section of this line is shown in Fig. 5. The same dielectric and conducting materials used for the rectangular line are used for this line.

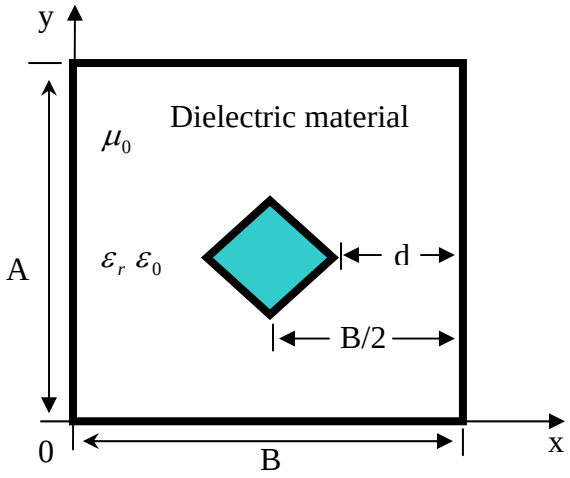

Figure 5. Cross-section of the diamondwise (or rhombus) structure with 45^o offset angle.

The following values are used for the COMSOL model of the line.
d = 1 mm
A= width of the outer conductor = 4 mm
B = height of the outer conductor = 4 mm

For the COMSOL model, we obtained the capacitance per unit line as 57.393 pF/m.

Table 3 displays the comparison of the characteristic impedance of several models. It is evident from the table that the results are in good agreement.

Table 3 Comparison of characteristic impedance Values of diamondwise structure.

Name	Z_0
Zheng et al. [18]	56.742
Bowan [24]	56.745
Riblet [27]	56.745
COMSOL [17]	58.079

D. A single-strip shielded transmission line

Figure 6 presents the cross section of a single-strip shielded transmission line.

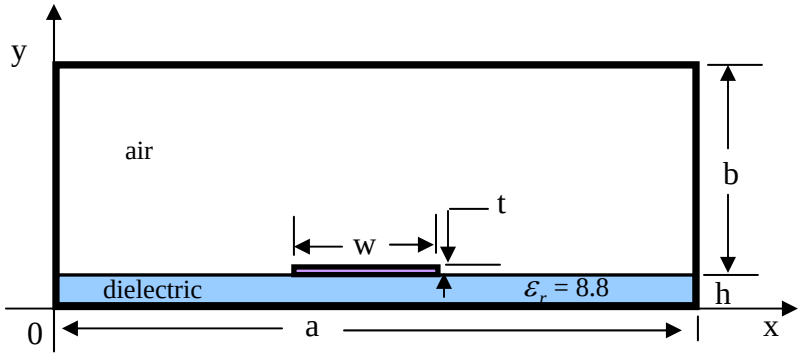

Figure 6. Cross-section of the single-strip shielded transmission line.

The following parameters are used in modeling the line. The characteristic impedance of such a lossless line is given by

$$Z = \frac{1}{c\sqrt{CC_o}} \qquad (2)$$

where

Z = characteristic impedance of the line
C_o = capacitance per unit length of the line when the substrate is replaced with air
C = capacitance per unit length of the line when the substrate is in place
c = 3 x 10^8 m/s (the speed of light in vacuum)

For COMSOL, the simulation was done twice on Figure 6 (to find C_o and C) using the following values.

Air:
ε_r =1, μ_r =1, σ = 0 S/m
Dielectric material:

ε_r = 8.8, μ_r =1, σ = 0 S/m
Conducting material:
ε_r =1, μ_r =1, σ = 5.8 x 10^7 S/m (copper)

w = width of the inner conductor = 1 mm
t = height of the inner conductor = 0.1 x 10^{-4} m
h = height of dielectric material = 1 mm
a = width of the outer conductor = 19 mm
b = height of the air-filled region = 9 mm

Using COMSOL for modeling and simulation of the lines involves taking the following steps:

1. Develop the geometry of the line, such as shown in Fig. 7.

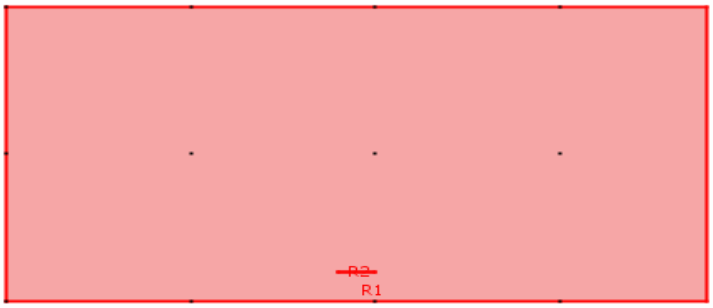

Figure 7. Geometry of a single-strip shielded transmission line at air.

2. We take the difference between the conductor and dielectric material.
3. We select the relative permittivity as 1 for the difference in step 2.
4. For the boundary, we select the outer conductor as ground and inner conductor as port.
5. We generate the finite element mesh, and then we solve the model and obtain the potential.
6. As postprocessing, we select Point Evaluation and choose capacitance element 11 to find the capacitance per unit length of the line.
7. We add a dielectric region under the inner conductor with relative permittivity as 8.8, as in Fig. 8. Then we take the same steps from 3 to 6 to generate the mesh as in Fig. 8. and the potential distribution as in Fig. 9.

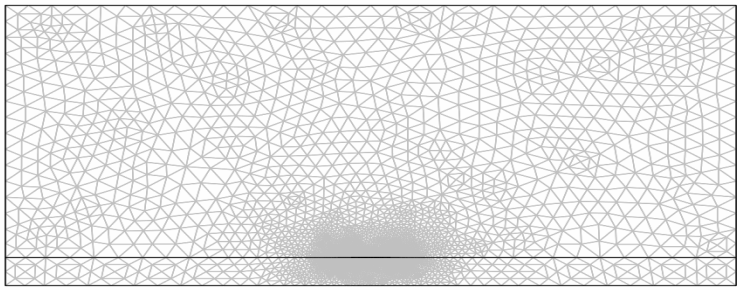

Figure 8. Mesh of the of a single-strip shielded transmission line.

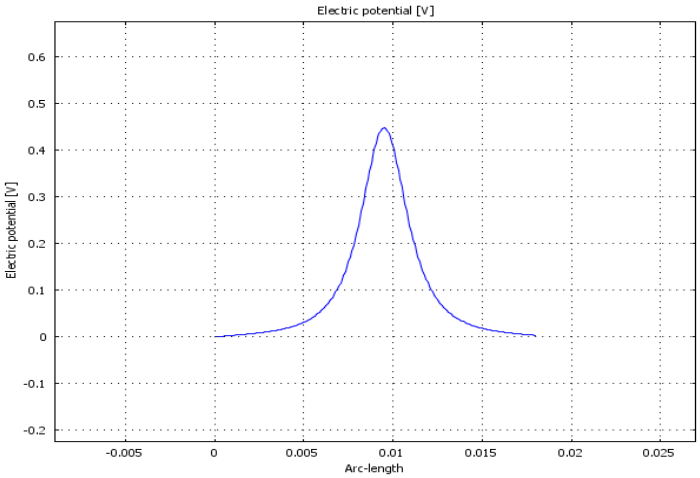

Figure 9. The potential distribution along y = 0.002.

Table 4 shows the comparison between our method using COMSOL and other methods. It is evident that the results are very close.

Table 4 Comparison of capacitance values for a single-strip shielded transmission line.

Methods	C_o **(pF/m)**	C **(pF/m)**
Finite difference method [7]	26.79	1405.2
Extrapolation [7]	26.88	1393.6
Analytical derivation [7]	27.00	1400.9
COMSOL [17]	26.87	1574.0

MULTISTRIP TRANSMISSION LINES

Recently, with the advent of integrated circuit technology, the coupled microstrip transmission lines consisting of multiple conductors embedded in a multilayer dielectric medium have led to a new class of microwave networks. Multiconductor transmission lines have been utilized as filters in microwave region which make it interesting in various circuit components. For coupled multiconductor microstrip lines, it is convenient to write [28-29]:

$$Q_i = \sum_{j=1}^{m} C_{sij} V_j \qquad \text{(i = 1, 2, ….., m)} \qquad (3)$$

where Q_i is the charge per unit length, V_j is the voltage of j th conductor with reference to the ground plane, C_{sij} is the short circuit capacitance between i th conductor and j th conductor. The short circuit capacitances can be obtained either from measurement or from numerical computation. From the short circuit capacitances, we obtain

$$C_{ii} = \sum_{j=1}^{m} C_{sij} \qquad (4)$$

where C_{ii} is the capacitance per unit length between the i th conductor and the ground plane. Also,

$$C_{ij} = -C_{sij}, \qquad j \neq i \tag{5}$$

where C_{ij} is the coupling capacitance per unit length between the i th conductor and j th conductor. The coupling capacitances are illustrated in Fig. 10.

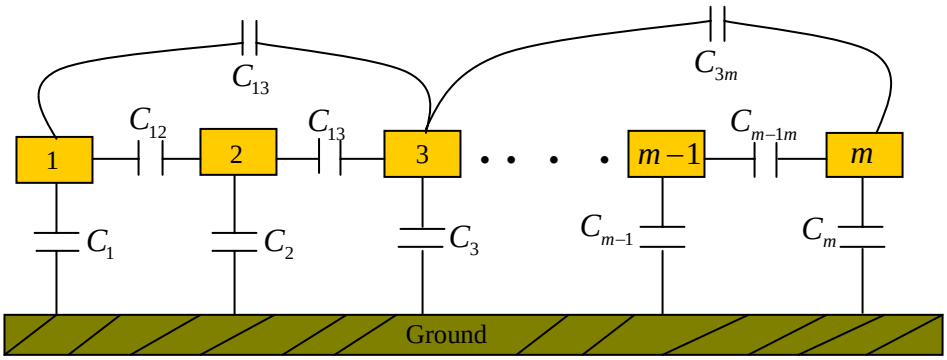

Figure 10. The per-unit length capacitances of a general m -conductor transmission line.

For m -strip line, the per-unit-length capacitance matrix is given by [30]

$$C = \begin{bmatrix} C_{11} & -C_{12} & \cdots & -C_{1m} \\ -C_{21} & C_{22} & \cdots & -C_{2m} \\ \vdots & \vdots & & \vdots \\ -C_{m1} & -C_{m2} & \cdots & C_{mm} \end{bmatrix} \tag{6}$$

Also, we can determine the characteristic impedance matrix for m -strip line by using [30]

$$Z_o = \begin{bmatrix} Z_{11} & Z_{12} & \cdots & Z_{1m} \\ Z_{21} & Z_{22} & \cdots & Z_{2m} \\ \vdots & \vdots & & \vdots \\ Z_{m1} & Z_{m2} & \cdots & Z_{mm} \end{bmatrix} \tag{7}$$

where Z_o is the characteristic impedance per unit length.

Using COMSOL for modeling and simulation of the lines involves taking the following steps:

1. Develop the geometry of the line.
2. We take the difference between the conductor and dielectric material
3. We select the relative permittivity as 1 for the difference in step 2.
4. We add a dielectric region under the inner conductors with specified relative permittivity.

5. For the boundary, we select the outer conductor as ground and the inner conductors as ports.
6. We generate the finite element mesh, and then we solve the model.
7. As postprocessing, we select Point Evaluation and choose capacitance elements to find the coupling capacitance per unit length of the line.
These steps were taken for the following four cases.

A. Double-strip shielded transmission line

Figure 11 presents the cross section of double-strip shielded transmission line, which consists of two inner conductors.

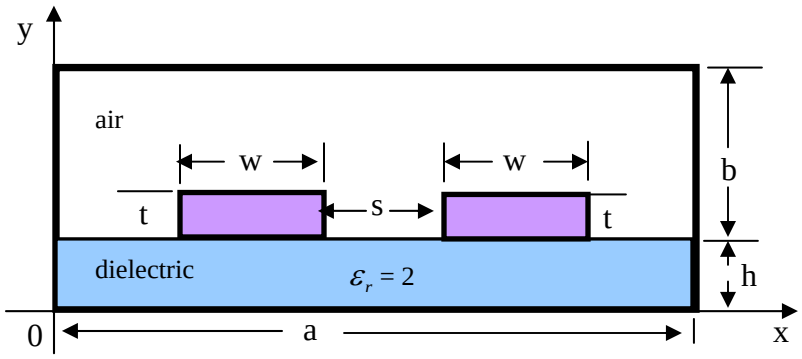

Figure 11. Cross-section of the double-strip shielded transmission line.

For COMSOL, the simulation was done twice on Figure 11 (one for C_o and other for C) using the following values.

Air:
ε_r =1, μ_r =1, σ = 0 S/m

Dielectric material:
ε_r = 2, μ_r =1, σ = 0 S/m

Conducting material:
ε_r =1, μ_r =1, σ = 5.8 x 10^7 S/m (copper)

For the geometry (see Fig. 11), we followed [11] and used for the following values:

w = width of each of the inner conductors = 3 mm
t = height (or thickness) of the inner conductors = 1 mm
s = distance between the inner conductors = 2mm
h = height of dielectric material = 1 mm
a = width of the outer conductor = 11 mm
b = height of the air-filled region = 2.7 mm

From the COMSOL model, the simulation was done twice – one for the case in which the line is air-filled (the dielectric was replaced by air) and the other case in which the dielectric is in place as shown in Fig. 11. Figure 12 shows the finite element mesh while Fig. 13 depicts the potential distribution for the dielectric case. The potential distribution for y = 1mm is portrayed in Fig. 14.

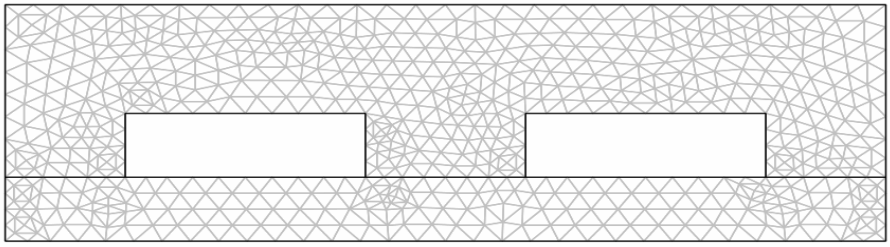

Figure 12. Mesh the of double-strip shielded transmission line.

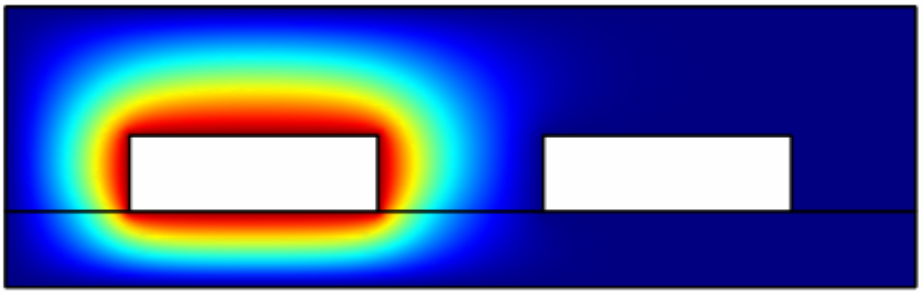

Figure 13. Potential distribution.

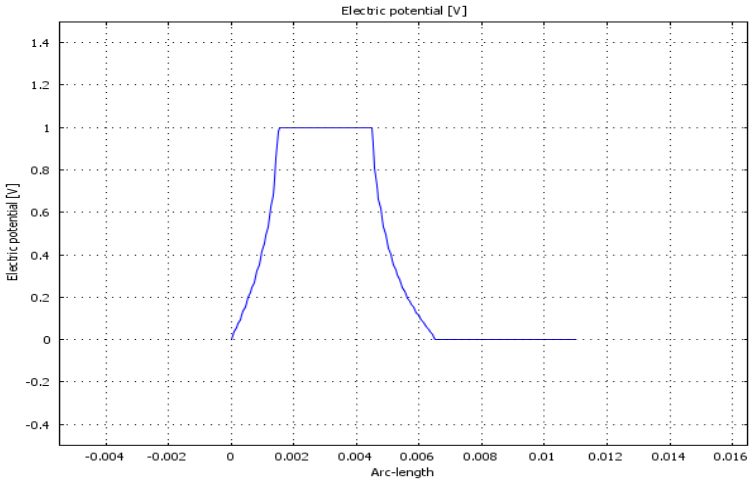

Figure 14. Potential distribution at y =1 mm.

We obtained the capacitances per unit length (C_o and C) by taking steps enumerated above for the single-strip transmission line. The results are shown in Tables 2 and 3. Table 5 is for the case which the line is air-filled, i.e. the dielectric in Fig. 11 is replaced

by air. Table 6 is for the case in which the dielectric is in place. The results in Table 6 are compared with other methods and found to be close.

Table 5 Capacitance values for double-strip air-filled shielded transmission line.

Methods	$C_{11} = C_{22}$ **(pF/m)**	$C_{12} = C_{21}$ **(pF/m)**
COMSOL [17]	72.9	-4.591

Table 6 Comparison of capacitance values for double-strip shielded transmission line shown in Fig. 11.

Methods	$C_{11} = C_{22}$ **(pF/m)**	$C_{12} = C_{21}$ **(pF/m)**
Spectral-space domain method [10]	108.1	-4.571
Finite element method [11]	109.1	-4.712
Point-matching method [8]	108.8	-4.683
COMSOL [17]	108.5	-4.618

B. Three-strip line

Figure 15 shows the cross section for three-strip transmission line. For COMSOL, the simulation was done twice on Figure 15 (one for C_o and other for C) using the following values.

Air:
ε_r =1, μ_r =1, σ = 0 S/m

Dielectric material:
ε_r = 8.6, μ_r =1, σ = 0 S/m

Conducting material:
ε_r =1, μ_r =1, σ = 5.8 x 10^7 S/m (copper)

For the geometry (see Fig. 15), we used the following values:

a = width of the outer conductor = 13 mm
b = height of the free space region (air) = 4 mm
h = height of the dielectric region = 2 mm
w = width of each inner strip = 2 mm
t = thickness of each inner strip = 0.01 mm
D = distance between the outer conductor and the first strip = 2.5 mm
s = distance between two consecutive strips = 1 mm

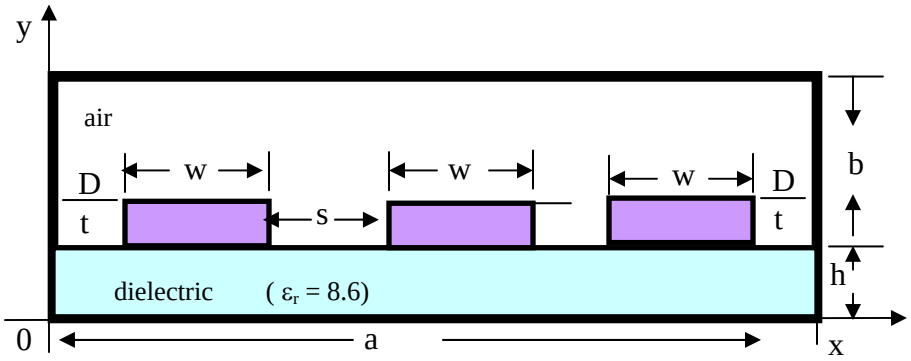

Figure 15. Cross-section of the three-strip transmission line.

Figure 16 shows the finite element mesh, while Fig. 17 illustrates the potential distribution along line y = h.

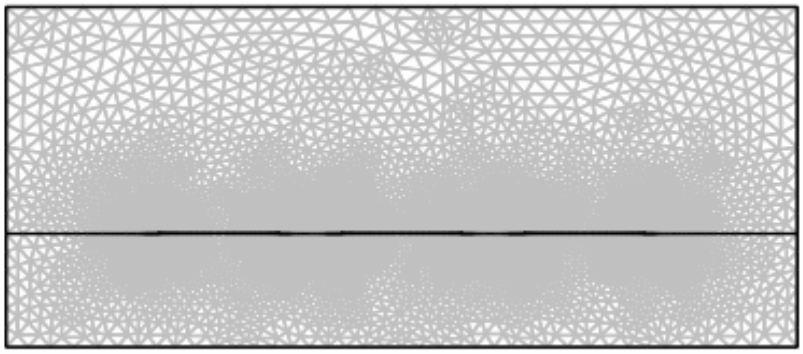

Figure 16. Mesh for the three-strip transmission line.

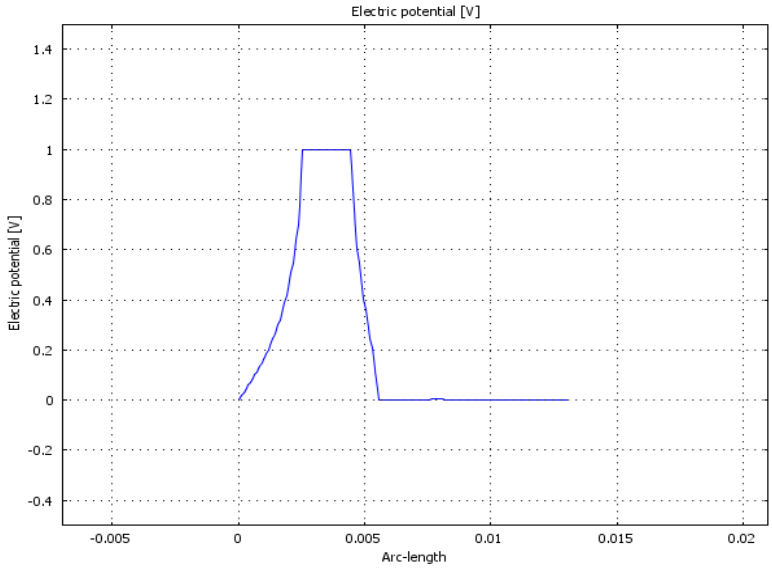

Figure 17. Potential distribution along the air-dielectric interface (y = h) for the three-strip transmission line.

Table 7 shows the finite element results for the three-strip line. Unfortunately, we could not find any work in the literature to compare our results.

Table 7 Capacitance values (in pF/m) for three-strip shielded microstrip line.

Methods	C_{11}	C_{21}	C_{31}
COMSOL [17]	163.956	-27.505	-0.4301

C. Six-strip line

Figure 18 shows the cross section for six-strip transmission line. For COMSOL, the simulation was done twice on Figure 18 (one for C_o and other for C) using the following values.

Air:
ε_r =1, μ_r =1, σ = 0 S/m

Dielectric material:
ε_r = 6, μ_r =1, σ = 0 S/m

Conducting material:
ε_r =1, μ_r =1, σ = 5.8 x 10^7 S/m (copper)

For the geometry (see Fig. 18), we used the following values:

a = width of the outer conductor = 15 mm

b = height of the free space region (air) = 2 mm
h = height of the dielectric region = 8 mm
w = width of each inner strip = 1 mm
t = thickness of each inner strip = 0.01 mm
D = distance between the outer conductor and the first strip = 2 mm
s = distance between two consecutive strips = 1 mm

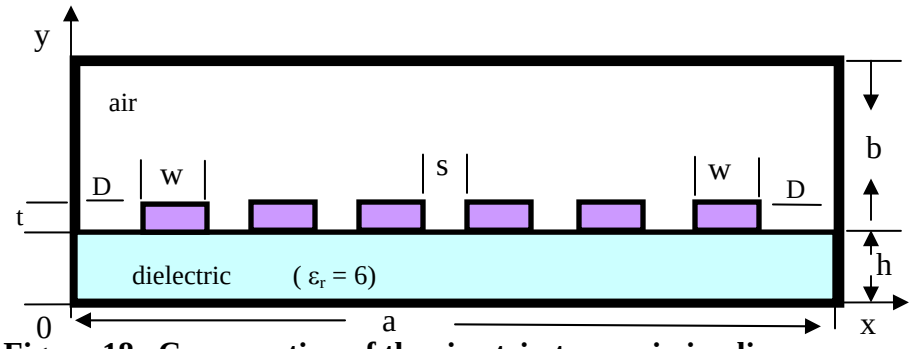

Figure 18. Cross-section of the six-strip transmission line.

Figure 19 shows the finite element mesh, while Fig. 20 depicts the potential distribution along line y = h.

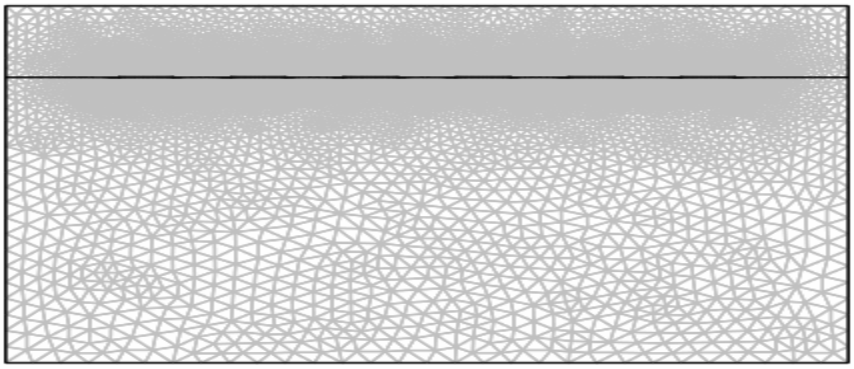

Figure 19. Mesh for the six-strip transmission line.

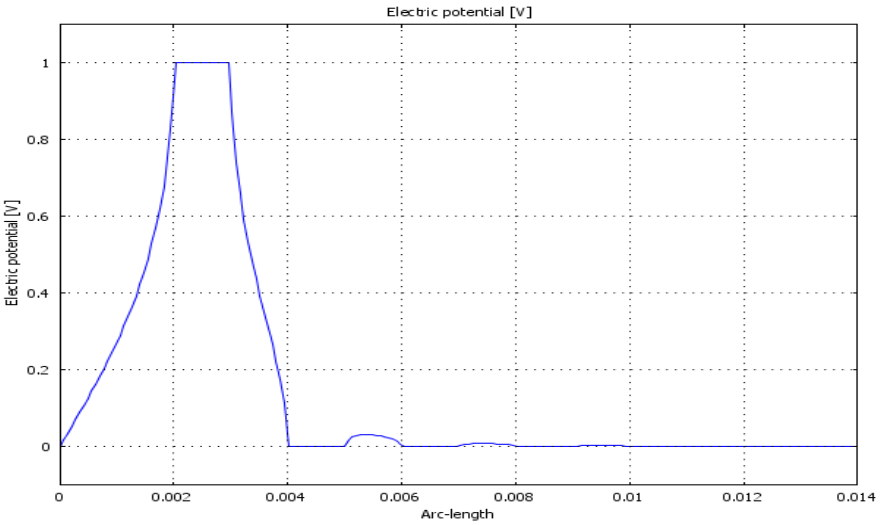

Figure 20. Potential distribution along the air-dielectric interface (y = h) for the six-strip transmission line.

The capacitance values for six-strip shielded microstrip line are compared with other methods as shown in Table 8, where "iterative" refers to an iterative method [30] and ABC refers to the asymptotic boundary condition [31]. It is evident from the table that the finite element methods based on [32] and [17] closely agree. The finite element methods seem to be more accurate than the iterative and ABC techniques. (The negative capacitances are expected from eq. (6)).

Table 8 Capacitance values (in pF/m) for six-strip shielded microstrip line.

Methods	C_{11}	C_{21}	C_{31}	C_{41}	C_{51}	C_{61}
Iterative [30]	66.8	– 27.9	– 5.49	– 2.08	– 0.999	– 0.704
Finite Element [32]	84.8	– 26.4	– 3.71	– 1.17	– 0.456	– 0.812
ABC [31]	68.6	– 31.5	– 6.00	– 2.25	– 0.792	– 0.602
COMSOL [17]	80.4	– 23.9	– 3.61	– 1.15	– 0.451	– 0.180

D. Eight-strip line

Figure 21 shows the cross section for eight-strip transmission line. For COMSOL, the simulation was done twice on Figure 21 (one for C_o and other for C) using the following values.

Air:
ε_r =1, μ_r =1, σ = 0 S/m

Dielectric material:
ε_r = 12.9, μ_r =1, σ = 0 S/m

Conducting material:
ε_r =1, μ_r =1, σ = 5.8 x 10^7 S/m (copper)

For the geometry (see Fig. 21), we used the following values:

a = width of the outer conductor = 175 mm
b = height of the free space region (air) = 100 mm
h = height of the dielectric region = 16 mm
w = width of each inner strip = 1 mm
t = thickness of each inner strip = 0.01 mm
D = distance between the outer conductor and the first strip = 80 mm
s = distance between two consecutive strips = 1 mm

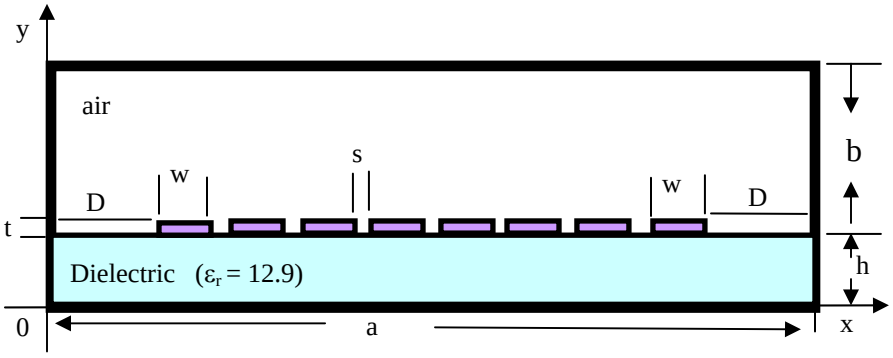

Figure 21. Cross-section of the eight-strip transmission line.

Figure 22 shows the finite element mesh, while Fig. 23 depicts the potential distribution along line y = 20mm.

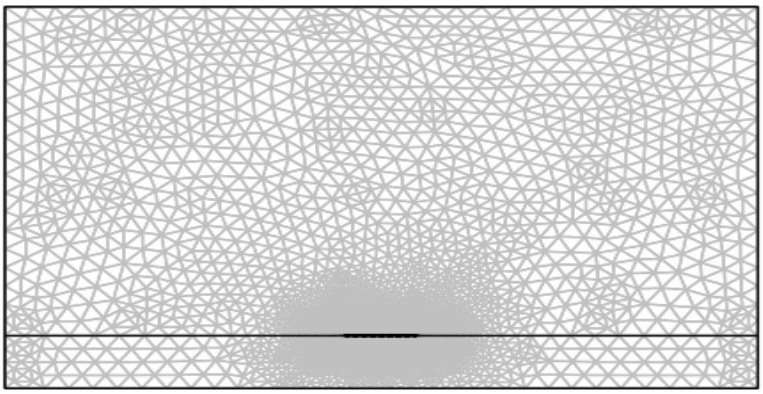

Figure 22. Mesh for the eight-strip transmission line.

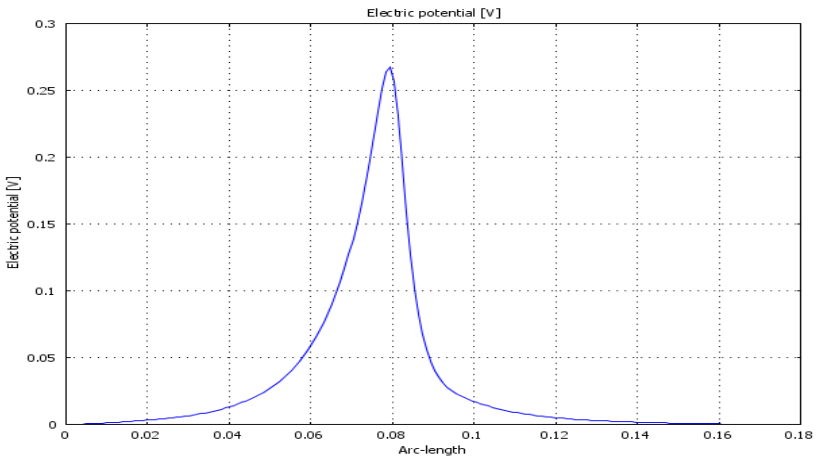

Figure 23. Potential distribution along the air-dielectric interface (y = 20 mm) for the eight-strip transmission line.

The capacitance values for eight-strip shielded microstrip line are compared with other methods as shown in Table 9, where other authors used analytic approach [33] and Fourier series expansion [34]. It is evident from the table that the results from finite element method (COMSOL) closely agree with the analytic approach.

Table 9 Capacitance values (in pF/m) for eight-strip shielded microstrip line.

Method	C_{11}	C_{21}	C_{31}	C_{41}	C_{51}	C_{61}	C_{71}	C_{81}
Analytic [33]	127.776	-58.446	-13.024	-5.721	-3.104	-1.892	-1.282	-1.211
Fourier series [34]	126.149	-57.066	-12.927	-5.684	-3.086	-1.875	-1.264	-1.185
COMSOL [17]	128.204	-58.759	-13.064	-5.739	-3.1206	-1.902	-1.290	-1.226

III. Conclusion

In this paper, we have presented simulations and models for rectangular coaxial lines as well as single-strip, double-strip, three-strip, six-strip, and eight-strip (multiconductor) shielded microstrip lines. Our simulations involved using COMSOL, a finite element package. We compared our results with other methods (finite difference, extrapolation, analytical derivation, spectral-space domain, and point-matching) and we found them be very close.

IV. References

[1] M. L. Crawford, "Generation of standard EM fields using TEM Transmission cells," *IEEE Transactions on. Electromagnetic Compatibility*, vol. EMC-16, pp. 189-195, Nov. 1974.

[2] J.R. Reid and R.T. Webster," A 60 GHz branch line coupler fabricated using integrated rectangular coaxial lines," *Microwave Symposium Digest, 2004 IEEE MTT-S International*, Vol. 2, pp.41 - 444 , 6-11 June 2004.

[3] S. Xu and P. Zhou, "FDTD analysis for satellite BFN consisting of rectangular coaxial lines,"*Asia Pacific Microwave Conference*, pp. 877-880, 1997.

[4] J. G. Fikioris, J. L. Tsalamengas, and G. J. Fikioris," Exact solutions for shielded printed microstrip lines by the Carleman-Vekua method", *IEEE Transactions on Microwave Theory and Techniques*, Vol. 37, No. 1, pp. 21-33, Jan. 1989.

[5] S. Khoulji and M. Essaaidi," Quasi-Static analysis of microstrip lines with variable-thickness substrates considering finite metallization thickness", *Microwave and Optic Technology Letters*, Vol. 33, No. 1, pp. 19-22, April. 2002.

[6] T.K. Seshadri, S. Mahapatra, and K. Rajaiah," Corner function analysis of microstrip transmission lines", *IEEE Transactions on Microwave Theory and Techniques*, Vol. 28, No. 4, pp. 376-380, April. 1980.

[7] S.V. Judd, I. Whiteley, R.J. Clowes, and D.C. Rickard," An analytical method for calculating microstrip transmission line parameters", *IEEE Transactions on Microwave Theory and Techniques*, Vol. 18, No. 2, pp. 78-87, Feb. 1970.

[8] N. H. Zhu, W. Qiu, E. Y. B. Pun, and P. S. Chung," Quasi-Static analysis of shielded microstrip transmission lines with thick electrodes", *IEEE Transactions on Microwave Theory and Techniques*, Vol. 45, No. 2, pp. 288-290, Feb. 1997.

[9] T. Chang and C. Tan," Analysis of a shielded microstrip line with finite metallization thickness by the boundary element method," *IEEE Transactions on Microwave Theory and Techniques*, Vol. 38, No. 8, pp. 1130-1132, Aug. 1990.

[10] G. G. Gentili and G. Macchiarella," Quasi-Static analysis of shielded planar transmission lines with finite metallization thickness by a mixed spectral-space domain method", *IEEE Transactions on Microwave Theory and Techniques*, Vol. 42, No. 2, pp. 249-255, Feb. 1994.

[11] A. Khebir, A. B. Kouki, and R. M. Mittra," Higher order asymptotic boundary condition for finite element modeling of two-dimensional transmission line structures", *IEEE Transactions on Microwave Theory and Techniques*, Vol. 38, No. 10, pp. 1433-1438, Oct. 1990.

[12] G. W. Slade and K. J. Webb," Computation of characteristic impedance for multiple microstrip transmission lines using a vector finite element method", *IEEE Transactions on Microwave Theory and Techniques,* Vol. 40, No. 1, pp. 34-40, Jan. 1992.
[13] M. S. Alam, K. Hirayama, Y. Hayashi, and M. Koshiba,"Analysis of shielded microstrip lines with arbitrary metallization cross section using a vector finite element method", *IEEE Transactions on Microwave Theory and Techniques,* Vol. 42, No. 11, pp. 2112-2117, Nov. 1994.
[14] J. Svacina," A new method for analysis of shielded microstrips", *Proceedings of Electrical Performance of Electronic Packaging,* pp. 111-114, 1993.
[15] H. Y. Yee, and K. Wu," Printed circuit transmission-line characteristic impedance by transverse modal analysis", *IEEE Transactions on Microwave Theory and Techniques,* Vol. 34, No. 11, pp. 1157-1163, Nov. 1986.
[16] I. P. Hong, N. Yoon, S. K. Park, and H. K. Park," Investigation of metal-penetrating depth in shielded microstrip line", *Microwave and Optic Technology Letters,* Vol. 19, No. 6, pp. 396-398, Dec. 1998.
[17] http://www.comsol.com/
[18] Q. Zheng, W. Lin, F. Xie, and M. Li,"Multipole theory analysis of a rectangular transmission line family," *Microwave and Optical Technology Letters,* Vol. 18, No. 6, pp. 382-384, Aug. 1998.
[19] T. S. Chen, "Determination of the Capacitance, Inductance, and Characteristic Impedance of Rectangular Lines," *IEEE Transactions on Microwave Theory and Techniques*, Volume 8, Issue 5, pp.510–519,Sep 1960.
[20] E. Costamagna and A. Fanni,"Analysis of rectangular coaxial structures by numerical inversion of the Schwarz-Christoffel transformation," *IEEE Transactions on Magnets,* Vol. 28, pp. 1454-1457, Mar. 1992.
[21] K. H. Lau," Loss calculation for rectangular coaxial lines," *IEE Proceedings,* Vol. 135, Pt. H. No. 3, pp. 207-209, June 1988.
[22] Personal computer program based on finite difference method.
[23] J. D. Cockcroft, "The effect of curved boundaries on the distribution of electrical stress round conductors," *J. IEE,* Vol. 66, pp. 385-409, Apr. 1926.
[24] F. Bowan," Notes on two dimensional electric field problems," *Proc. London Mathematical Society.,* Vol. 39, No. 211, pp. 205-215, 1935.
[25] H. E. Green," The characteristic impedance of square coaxial line," *IEEE Transactions Microwave Theory and Techniques,* Vol. MTT-11, pp. 554-55, Nov.1963.
[26] S. A. Ivanov and G. L. Djankov," Determination of the characteristic impedance by a step current density approximation," *IEEE Transactions on Microwave Theory and Techniques.,* Vol. MTT-32, pp. 450-452, Apr. 1984.
[27] H. J. Riblet, "Expansion for the capacitance of a square in a square with a comparison," *IEEE Transactions on Microwave Theory and Techniques,* Vol. 44, pp. 338-340, Feb. 1996.
[28] M. S. Lin, "Measured capacitance coefficients of multiconductor microstrip lines with small dimensions," *IEEE Transactions on Microwave Theory and Techniques,* vol. 13, no. 4, pp. 1050-1054, Dec. 1990.

[29] F. Y. Chang,"Transient analysis of lossless coupled transmission lines in a nonhomogeneous dielectric media," *IEEE Transactions on Microwave Theory and Techniques*, vol 18, no 9, pp. 616-626, Aug. 1970.

[30] P. N. Harms, C. H. Chan, and R. Mittra, "Modeling of planar transmission line structures for digital circuit applications," *Arch. Eleck. Ubertragung.*, vol. 43, pp. 245-250, 1989.

[31] A. Kherbir, A. B. Kouki, and R. Mittra, "Absorbing boundary condition for quasi-TEM analysis of microwave transmission lines via the finite element method," *J. Electromagnetic Waves and Appl*ications, vol. 4, no. 2, 1990.

[32] A. Khebir, A. B. Kouki, and R. Mittra, "High order asymptotic boundary condition for the finite element modeling of two-dimensional transmission line structures," *IEEE Transactions on Microwave Theory and Techniques*, vol. 38, no. 10, pp. 1433-1438, Oct. 1990.

[33] D. Homentcovschi, G. Ghione, C. Naldi, and R. Oprea," Analytic determination of the capacitance matrix of planar or cylindrical multiconductor lines," *IEEE Transactions on. Microwave Theory and Techniques*, pp. 363-373, Feb. 1995.

[34] M. K. Amirhosseini,"Determination of capacitance and conductance matrices of lossy shielded coupled microstrip transmission lines," *Progress In Electromagnetics Research*, PIER 50, pp. 267-278, 2005.